Title

Istradefylline reduces memory deficits in aging mice with amyloid pathology

Permalink

https://escholarship.org/uc/item/6bj3j6d6

Authors

Orr, Anna G
Lo, Iris
Schumacher, Heike
et al.

Publication Date

DOI

Peer reviewed

Istradefylline reduces memory deficits in aging mice with amyloid pathology

Anna G. Orr[a,b], **Iris Lo**[a], **Heike Schumacher**[a], **Kaitlyn Ho**[a], **Michael Gill**[a], **Weikun Guo**[a], **Daniel H. Kim**[a], **Anthony Knox**[a], **Takashi Saito**[c], **Takaomi C. Saido**[c], **Jeffrey Simms**[a], **Carlee Toddes**[a], **Xin Wang**[a], **Gui-Qiu Yu**[a], and **Lennart Mucke**[a,b,*]

[a]Gladstone Institute of Neurological Disease, San Francisco, CA 94158 USA

[b]Department of Neurology, University of California, San Francisco, CA 94158 USA

[c]Laboratory for Proteolytic Neuroscience, RIKEN Brain Science Institute, Wako, Saitama 351-0198, Japan

Abstract

Adenosine A_{2A} receptors are putative therapeutic targets for neurological disorders. The adenosine A_{2A} receptor antagonist istradefylline is approved in Japan for Parkinson's disease and is being tested in clinical trials for this condition elsewhere. A_{2A} receptors on neurons and astrocytes may contribute to Alzheimer's disease (AD) by impairing memory. However, it is not known whether istradefylline enhances cognitive function in aging animals with or without AD-like amyloid plaque pathology. Here, we show that elevated levels of Aβ, C-terminal fragments of the amyloid precursor protein (APP), or amyloid plaques, but not overexpression of APP per se, increase astrocytic A_{2A} receptor levels in the hippocampus and neocortex of aging mice. Moreover, in amyloid plaque-bearing mice, low-dose istradefylline treatment enhanced spatial memory and habituation, supporting the conclusion that, within a well-defined dose range, A_{2A} receptor blockers might help counteract memory problems in patients with Alzheimer's disease.

1. Introduction

Adenosine receptors regulate brain function and may have key roles in neurodegenerative disorders. Adenosine A_{2A} receptors (A_{2A}Rs) are highly expressed in inhibitory medium spiny neurons of the striatum and regulate the balance between the direct and indirect neural pathways controlling movement[1]. A_{2A}R blockers enhance motor function in animal models

of Parkinson's disease (PD). Istradefylline, a selective $A_{2A}R$ blocker, is safe and well-tolerated[2] and approved in Japan for the treatment of PD[3].

In animal models, $A_{2A}R$ blockade or removal ameliorated cognitive dysfunction resulting from acute brain trauma or seizures[4, 5]. $A_{2A}Rs$ expressed by neurons and astrocytes also contributed to cognitive deficits in models of Alzheimer's disease (AD)[6–12]. Furthermore, we previously found that $A_{2A}R$ levels on astrocytes were markedly increased in AD patients, and the increases correlated with disease severity[8]. Gene-expression profiling in postmortem human brains revealed that A_{2A} mRNA levels correlate positively with frontal cortex atrophy in late-onset AD[13]. Moreover, genetic ablation of $A_{2A}Rs$ in astrocytes enhanced reference memory in mice with or without AD-like plaque pathology[8], but impaired working memory in mice without plaques[14] supporting the notion that astrocytes regulate cognitive functions[15]. These findings also suggest that alterations in $A_{2A}R$ levels contribute to cognitive deficits in AD. However, it is uncertain what causes the increases in astrocytic $A_{2A}R$ levels in AD and whether $A_{2A}R$ antagonists can reduce cognitive deficits in the context of AD-like plaque pathology. Here, we analyzed $A_{2A}R$ expression in APP transgenic mice with or without plaque pathology and assessed the effects of istradefylline on the behavior of plaque-bearing mice.

2. Materials and methods

2.1. Animals

Mice were housed in the Gladstone animal facility and treated in accordance with guidelines of the Institutional Animal Care and Use Committee, University of California, San Francisco. Mice were housed in groups of 2–5 per cage and maintained on a 12-h light/dark cycle with *ad libitum* access to food (PicoLab Rodent Diet 20, LabDiet, 5053) and water. All experiments were conducted during the light cycle and included littermate controls. Male and female littermates were randomly assigned to a drug treatment condition and were balanced for age and sex as much as possible within each available cohort. Mice were treated, monitored and tested by experimenters blinded to the genotypes and treatment conditions. hAPP-J20 mice (C57BL/6, line J20) express an alternatively spliced human *APP* minigene encoding hAPP695, hAPP751 and hAPP770 with the Swedish and Indiana familial AD mutations directed by the *PDGF*β-chain promoter[16, 17]. hAPP-I5 mice (C57BL/6, line I5) express a human *APP* minigene directed by the *PDGF*β-chain promoter that encodes wildtype hAPP695, hAPP751 and hAPP770 without familial AD mutations[16]. Homozygous *APP* knock-in (APP^NL-G-F) mice have two mouse *App* alleles bearing the Swedish, Beyreuther/Iberian and Arctic familial AD mutations as well as a humanized Aβ sequence[18]. This study was approved by the Institutional Animal Care and Use Committee, and all experiments were conducted in accordance with the United States Public Health Service's Policy on Humane Care and Use of Laboratory Animals.

2.2. Drug preparation and administration

Istradefylline was obtained in powder form (Tocris, 5147) and is highly insoluble in water. To enable daily oral intake of istradefylline in the drinking water, we tested a variety of solubilizing agents. We found that istradefylline was not fully solubilized and gradually

precipitated in solutions with less than 30% DMSO or in 0.25–1% methylcellulose. Although a mixture of 40% DMSO and 60% Cremophor EL (Sigma) effectively solubilized the drug, daily fluid intake of the final treatment solution was reduced in mice, possibly due to the odor of Cremophor EL. We therefore reduced the amount of Cremophor EL by substitution with mineral oil. The final formulation for solubilizing the drug consisted of 40% DMSO, 30% Cremophor EL and 30% mineral oil. The solubilized drug stock was further diluted in 2% sucrose in water to prepare the final treatment solutions, which contained 0.2–2% DMSO, 0.15–1.5% Cremophor EL, and 0.15–1.5% mineral oil, depending on the specific drug dose. We used low concentrations of DMSO and the amounts that reached the brain after ingestion were likely much lower[19]. However, because DMSO can affect various biological processes, including AD-linked cascades[20], the vehicle solutions contained the same final concentrations of solubilizing agents and sucrose as the drug solutions, but did not contain istradefylline.

All final solutions were prepared daily and were protected from light with aluminum foil. Mice received drug or vehicle solutions in 50-ml tubes with attached spouts placed in their home cages and did not have access to other sources of fluids during treatment, which continued for the duration of behavioral testing. Body weight, chow intake and daily fluid intake were closely monitored (Suppl. Figs. 9–10). To habituate the mice to the bottles and the vehicle solutions, the mice were first given bottles with plain water for 2–3 days followed by vehicle solution for another 2–3 days. Subsequently, half of the mice were given bottles with vehicle solution containing istradefylline. The route of administration and dosing were chosen based on the drug's pharmacokinetic properties[21] and previous studies[4]. To achieve the desired drug dose in male and female mice, average body weight and daily fluid intake were used to calculate the required drug concentrations in the solutions.

For cohorts receiving 4 or 40 mg/kg/day, open-field experiments were started 1–3 days after drug treatment was initiated. For cohorts receiving 10 or 15 mg/kg/day, open-field experiments were started two weeks after drug treatment was initiated. The longer time-points were designed to eliminate the potential confound of behavioral testing before steady-state drug levels were reached. All Morris water maze (MWM) experiments were performed three weeks after drug treatment was initiated. Mice were tested in the elevated plus maze and the Rotarod two and five weeks after treatment was initiated, respectively.

To measure istradefylline levels in the plasma and brain, mice were treated with drug or vehicle as indicated, anesthetized with Avertin (tribromoethanol, 250 mg/kg) and perfused transcardially with 0.9% saline for 1 min. Cardiac blood was collected in anesthetized mice immediately before perfusion. The plasma was isolated by centrifugation at 3000 rpm for 15 min at 4°C. Istradefylline concentrations in the plasma and snap-frozen hemibrains were measured by Brains Online using HPLC with tandem mass spectrometry and internal standards. Notably, istradefylline isomerizes when exposed to light[22]. Indeed, the chromatograms showed two peaks for istradefylline. Calculations for each peak were made assuming that the racemic mixture consisted of equal parts of each isomer. E isomers may have higher adenosine receptor affinity than Z isomers[23]. The reported concentrations are the sum of the two isomers. Non-terminal blood collection was performed by submandibular bleeding in mice under brief chloroform anesthesia.

We performed a pilot dosing study in 9–16-month-old NTG male and female C57Bl/6 mice, which showed that oral intake of istradefylline resulted in dose-dependent increases in plasma levels of the drug by days 3 and 8 (Suppl. Fig. 1A). Approximately 75% of fluid intake in C57Bl/6 mice occurs during the dark phase[24], which might be expected to cause reductions in the levels of drug during the light phase. However, we did not observe reductions in plasma drug levels in the late afternoon (approximately 4 PM) as compared to the morning (approximately 9 AM) (Suppl. Fig. 1A), suggesting that drug levels were relatively stable throughout the day. Istradefylline treatment at 40 mg/kg/day for 25 days resulted in comparable plasma drug levels in 18–19-month-old NTG and hAPP mice (Suppl. Fig. 1B). Following a 10-day washout period, the levels of drug in the plasma were markedly reduced (Suppl. Fig. 1B). Chronic treatment with 4–15 mg/kg/day resulted in dose-dependent increases in the levels of drug in brain tissue in WT and hAPP mice (Suppl. Fig. 1C).

2.3. Behavioral testing

For all behavioral testing, the experimenters were blinded to the genotype and treatment of the mice. Mice that showed poor health or injuries that interfered with behavioral testing (for example, skin lesions, eye injury, tumors, slowed movement or inability to swim) were excluded from the analyses. The incidence of such health problems was not different between drug-treated and placebo-treated mice (data not shown). Behavioral data were obtained with the help of the Gladstone Institutes' Neurobehavioral Core.

2.4. Morris water maze

The maze consisted of a 122-cm-diameter pool filled with water (20 ± 2 °C) made opaque with nontoxic white tempera paint. The pool was surrounded with distinct extra-maze cues. Before hidden platform training, all mice underwent one session of 3–4 pre-training trials in which they swam in a rectangular channel (15 cm × 122 cm) and mounted a square platform (14 × 14 cm) hidden 1 cm below the water surface in the middle of the channel. If a mouse did not mount the platform within 10 s, it was guided to the platform by the experimenter and was allowed to sit on the platform for 10 s before it was removed by the experimenter. The day after pre-training, mice were trained in the circular water maze. For hidden platform training, the platform was submerged 1.5 cm below the surface. The platform location remained the same throughout training, but the drop location varied randomly between the four daily trials. Mice received two sessions per day (3-h interval between sessions) for 8 consecutive days. Each session consisted of two trials with a 15-min interval. The maximum time allowed per trial was 60 s. If a mouse did not find or mount the platform, it was guided to the platform by the experimenter. All mice were allowed to sit on the platform for 15 s after each training trial.

For probe trials, the platform was removed and each mouse was allowed to swim for 60 s. The drop location for the probe trials was 180° from the platform location used during hidden platform training. After 60 s, mice were guided to the platform location before removal from the pool. Mice were probed on days 1 and 3 after hidden platform training. After probe testing, cued (visible) platform training was performed using a new platform location and a clearly visible cue (a 15-cm pole on top of the platform). Mice received three

sessions of two cued trials per session in one day (10-min interval between trials and 2-h interval between sessions). All behavior was recorded and analyzed with an Ethovision XT video tracking system (Noldus). Escape latencies, distance traveled, swim paths, swim speeds, platform crossings and proximity to the platform were recorded automatically for subsequent analysis.

2.5. Open-field test

Spontaneous movement, rearing and context-dependent habituation in the open field were measured with an automated Flex-Field/Open Field Photobeam Activity System (San Diego Instruments, San Diego, CA). After acclimation to the testing room for 1 h, mice were placed individually in a clear plastic chamber ($41 \times 41 \times 30$ cm) with two 16×16 photobeam arrays detecting horizontal and vertical movements. Chambers were surrounded by distinct proximal cues. Mice were exposed to the chambers in 5-min trials (2 trials per day with a 3-h inter-trial interval) and tested in the same chambers 3–5 weeks later. The apparatus was cleaned with 70% alcohol after each mouse. Total movements (ambulations), rearings, and time spent in the center versus periphery of the open field were recorded automatically by the system for subsequent analysis.

2.6. Elevated plus maze

The maze consisted of two open and two enclosed arms elevated 63 cm above the ground (Hamilton-Kinder, Poway, CA). After acclimation to the testing room for 1 h, mice were placed at the junction between the open and closed arms of the maze and allowed to explore freely for 5 min. The maze was cleaned with 70% ethanol after each mouse. Total distance traveled and time spent in the open and closed arms were recorded automatically for subsequent analysis.

2.7. Rotarod test

After acclimation to the testing room for 1 h, mice were placed on the Rotarod (Med Associates Inc.), which was rotated at a constant speed of 16 rpm on day 1 and at increasing speeds (4–40 rpm) on day 2. Photobeam interruptions caused by mice falling off the rotating rod were recorded. Photobeams were interrupted by the experimenter if the mouse held onto the rod without walking for three full rotations. Each mouse was given three trials with a 10-min inter-trial interval and a maximum of 300 s per trial. The average latency to fall off the Rotarod was calculated.

2.8. Immunohistochemistry

Mice were anesthetized with Avertin (tribromoethanol, 250 mg per kg) and perfused with 0.9% saline for 1 min. Brains were removed, post-fixed in 4% paraformaldehyde, incubated in 30% sucrose for 1–3 days at 4°C, and sectioned at a thickness of 30 μm using a freezing microtome (Leica SM 2000R). Sections were incubated for 15 min in 0.3% Sudan black (Sigma-Aldrich) with 70% ethanol to block auto-fluorescence and for 2 h in blocking reagent provided in the mouse-on-mouse kit (Vector Laboratories). Sections were then incubated overnight at room temperature in mouse anti-A_{2A} receptor IgG2a antibody (1:200, Millipore, 05-717), mouse anti-GFAP IgG1 antibody (1:1000, Millipore, MAB360), and

rabbit anti-human amyloid-β (N) IgG antibody (1:250, IBL-America, 18584), followed by a 1-h incubation at room temperature with goat anti-mouse IgG2a-488, goat anti-mouse IgG1-546 and goat anti-rabbit IgG-648. Sections were mounted onto slides with Prolong Diamond anti-fade reagent (Thermo Fisher Scientific). Selectivity of the A_{2A} receptor antibody was confirmed using brain sections from A_{2A} knockout mice, as reported previously[8].

Brain sections were imaged using a 10X objective (Keyence) and analyzed with a BZ-9000 automated microscope system and analysis application (Keyence). A_{2A} and GFAP immunoreactivities were quantified in the stratum radiatum of the CA1 region of the dorsal hippocampal formation and in the somatosensory cortex using two sections per mouse. A_{2A} receptor and GFAP immunoreactivities were also observed in the dorsal hippocampus (data not shown). To obtain high-resolution photomicrographs, multiple images were acquired and reconstructed automatically for each brain section. After cropping the images to isolate the CA1 and somatosensory cortex, thresholding was carried out using a constant intensity value to separate background staining from the signal of interest. Regions of interest were automatically visualized and quantified to obtain the total area of the cropped region and the total area of immunoreactivity per section. These values were averaged per mouse and compared between genotypes.

2.9. Statistics

Unless indicated otherwise, data are presented as means ± SEM. All statistical tests except for the data shown in Fig. 2A were performed with GraphPad Prism (version 5). In Fig. 2A, the learning curves were analyzed using rank-summary scoring and linear regression[25] in R software[26]. Sample sizes were determined based on pilot experiments and previous studies including similar types of experiments. Normality was tested by D'Agostino and Pearson omnibus normality test. The criterion for data point exclusion was established during the design of the study and was set to values above or below two standard deviations from the group mean. We excluded 7 mice (5 NTG and 2 hAPP mice) from behavioral testing due to sporadic health issues, such as eye damage and skin lesions. Variances were compared by F test or Bartlett's test. Differences between two groups were assessed by unpaired two-tailed Student's *t* test and FDR correction for multiple comparisons. Welch's correction was used to account for unequal variances between two groups. Differences among treatment groups were assessed by one-way or two-way ANOVA followed by Dunnett's or Bonferroni post-test, respectively.

3. Results

Similar to AD patients, human amyloid precursor protein (hAPP) transgenic mice from line J20 form amyloid plaques and show progressive increases in astrocytic $A_{2A}R$ levels[8]. These mice overexpress familial AD-mutant forms of hAPP in neurons and have pathologically elevated cerebral levels of amyloid-β (Aβ), the main constituent of amyloid plaques, and other AD-like abnormalities[27, 28]. The close temporal and spatial association between amyloid deposition and astrocytic $A_{2A}R$ expression suggests that the latter may be caused by amyloid plaques, similar to other plaque-associated changes observed in AD[29].

Alternatively, the increase in astrocytic A_{2A}Rs may be caused by overexpression of hAPP together with biological aging or the passage of time[30]. To test this alternate hypothesis, we studied hAPP mice from line I5, which overexpress wildtype hAPP and never form amyloid plaques[16], and *App* knock-in (APP[NL-G-F]) mice, which do not overexpress hAPP or mouse APP but—like hAPP-J20 mice—overproduce amyloidogenic human Aβ and the C-terminal APP fragment C99, form amyloid plaques, and develop astrocytosis and memory loss[18, 31] (and data not shown).

Like hAPP-J20 and hAPP/PS1 mice[8], plaque-bearing APP[NL-G-F] mice had increased levels of glial fibrillary acidic protein (GFAP), indicating reactive astrocytosis, and increased astrocytic A_{2A}R levels in the hippocampus and neocortex; these increases were not found in hAPP-I5 mice (Fig. 1). Thus, hAPP overexpression per se did not cause the astrocytic alterations. Since hAPP-J20 and APP[NL-G-F] mice have normal astrocytic A_{2A}R levels before they form amyloid plaques[8] (and data not shown), accumulation of amyloid plaques is the likeliest cause of increased astrocytic A_{2A}R expression in these models and, possibly, also in the human condition. We cannot rule out contributions from pathologically elevated levels of soluble Aβ assemblies (particularly oligomers) or from increased C99 levels, which occur in hAPP-J20 and APP[NL-G-F] mice and in humans with some familial forms of AD[32]. Indeed, application of $Aβ_{1-42}$ increased the levels of A_{2A}R in primary astrocyte cultures[33]. Furthermore, APP metabolites are not the only factors that can increase astrocytic A_{2A}R expression[8].

In 14–21-month-old wild-type (WT) nontransgenic mice and hAPP-J20 mice, administration of istradefylline in the drinking water caused dose-dependent increases of drug levels in plasma and brain (Suppl. Fig. 1). In pilot experiments, doses higher than 10 mg/kg/day increased total movements and rearing in both genotypes (Suppl. Fig. 2), consistent with reports that istradefylline enhances locomotion[34, 35]. To avoid this potential confound, mice were treated with 4 or 10 mg/kg/day.

The effects of istradefylline on learning and memory were tested with the Morris water maze. To escape the water, mice must learn to use extramaze visual cues to locate a hidden platform[36]. After training, the platform is removed and probe trials are done to assess spatial memory. Three weeks of drug treatment at either dose did not affect learning in training trials (Fig. 2A; Suppl. Fig. 3A). In probe trials 1 day after training, hAPP mice treated with 10 mg/kg/day spent more time in the target quadrant (Fig. 2B) than vehicle-treated hAPP mice and achieved better average proximity to the platform location (Fig. 2C), a sensitive measure of spatial memory[25, 37, 38].

As shown by proximity to platform location, vehicle-treated hAPP mice had the most prominent deficits during the first 20 seconds of the probe trial relative to vehicle-treated WT mice (Fig. 2D and G; Suppl. Figs. 3B and 5C), possibly because their search strategy improved with time. Since the platform was no longer at the expected location, learning-dependent extinction or changes in the search strategy of WT mice may have contributed also[37]. hAPP mice treated with 4 or 10 mg/kg/day performed better than vehicle-treated hAPP mice during the first 20 seconds of the probe trial (Fig. 2E; Suppl. Fig. 3C). In a second probe trial 3 days after training, hAPP mice treated with 10 mg/kg/day again showed

enhanced performance (Fig. 2G, H). Drug-treated hAPP mice also had faster swim speeds than vehicle-treated hAPP mice (Fig. 2F and I). However, drug treatment did not affect swim speeds during training (Suppl. Fig. 4A) or enhance motor performance in the Rotarod test (Suppl. Fig. 4B, C), suggesting that the treatment did not increase locomotor function per se.

At 15 mg/kg/day, istradefylline did not affect learning (Suppl. Fig. 5A) but impaired probe performance of WT mice and did not improve the performance in hAPP mice (Suppl. Fig. 5B–F). Thus, in aging mice with chronic plaque pathology, istradefylline enhances spatial memory primarily at low doses.

Istradefylline at doses of 4, 10 and 15 mg/kg/day also improved learning of the cued navigation task in hAPP mice (Suppl. Fig. 6), possibly due to improvements in striatum-dependent navigation to the visible platform[39]. In contrast, istradefylline treatment did not affect performance during hidden platform training (Fig. 2A; Suppl. Figs. 3A and 5A), which involves distal cues and is dependent on hippocampal function.

We also examined the effects of istradefylline in the open-field test, in which mice were habituated to an arena by repeated exposures. At 4 mg/kg/day, istradefylline enhanced context habituation in WT and hAPP mice (Suppl. Fig. 7A, B), which provides another putative measure of learning and memory[40]. Three weeks after habituation, drug-treated WT and hAPP mice still showed fewer movements in the familiar context (Suppl. Fig. 7C). At 10 mg/kg/day, istradefylline had similar effects (Suppl. Fig. 7E, F). Decreased locomotion has been reported for chronic intake of caffeine[41], a nonselective adenosine receptor blocker, and genetic deletion of the $A_{2A}R$[42, 43], but—to our knowledge—not yet for istradefylline or other selective $A_{2A}R$ antagonists.

Istradefylline did not affect time spent in the center of the open field (Suppl. Fig. 7D) and increased the amount of time spent in the open arms of the elevated plus maze (Suppl. Fig. 8), suggesting that istradefylline did not increase anxiety-like behaviors. Thus, besides enhancing spatial memory and cued navigation in aging hAPP mice, $A_{2A}R$ blockade improved context habituation without reducing motor ability or increasing anxiety.

4. Discussion

Our findings suggest that amyloid deposition is a strong causal driver of the striking increase in astrocytic $A_{2A}R$ expression we previously discovered in AD patients and a related animal model[8]. We also demonstrate that istradefylline treatment can improve memory in the context of AD-related plaque pathology in aging mice. Notably, this beneficial effect was observed at relatively low doses, whereas a higher dose had no effect on probe performance in plaque-bearing mice. Interestingly, other memory-enhancing agents such as cholinergic and noradrenergic agonists also had U- or J-shaped dose-response curves in different species and behavioral paradigms[44]. Caffeine, a nonselective blocker of $A_{2A}R$, had various beneficial effects in animal models of amyloid pathology and enhances memory consolidation in humans[45–47]. In light of these findings, the use of istradefylline in the treatment of PD patients and ongoing trials with other $A_{2A}R$ blockers, it would be

interesting to determine whether these drugs could also improve cognitive functions in patients with AD.

Like other neurotherapeutics, istradefylline had a narrow therapeutic window in our study, showing beneficial effects in aging mice only at doses 10 mg/kg/day. In a nonhuman primate model of PD, istradefylline also reduced cognitive deficits only at the lowest dose[48]. Age and other variables can shift therapeutic windows[49]. Similar shifts during AD might require patient stratification and dose adjustments based on biomarkers and end points that correlate with drug efficacy[50]. Molecular imaging of aberrant increases in $A_{2A}R$ levels and drug occupancy in extrastriatal regions of the brain, particularly the hippocampus, with radiopharmaceutical ligands and PET scanning[51, 52] might be used to select patients and guide adaptive dosing. These strategies could also help identify the stage(s) when $A_{2A}R$ blockers might be most effective in AD. Our results in transgenic mice and AD patients suggest that $A_{2A}R$ receptor levels in astrocytes closely relate to plaque pathology and disease stage (this study and ref. 8), although a variety of additional factors might affect when and how astrocytes, neurons and other cell types express these receptors in AD.

As discussed previously[53, 54], low doses of $A_{2A}R$ antagonists may cause a different set of behavioral effects than high doses by engaging different neural systems or the same neural systems in a different manner. Indeed, low-dose (4 or 10 mg/kg/day) istradefylline treatment enhanced habituation and spatial memory without increasing movements in aging hAPP mice, whereas the 15 mg/kg/day dose elicited modest alterations in locomotion and the 40 mg/kg/day dose triggered robust hyperlocomotion. These results are consistent with previous studies demonstrating different dose-dependent effects of $A_{2A}R$ antagonists in animal models of striatal damage[55, 56].

In healthy brains, $A_{2A}Rs$ are most highly expressed by striatal inhibitory neurons and moderately expressed by other neurons[57]. The striatum is critical for movement control, and genetic ablation of $A_{2A}Rs$ in inhibitory neurons prevents istradefylline-induced hyperactivity[58]. Intriguingly, ablation of $A_{2A}Rs$ in inhibitory neurons worsened probe performance without affecting learning[59]. Thus, blockade of $A_{2A}Rs$ on inhibitory neurons might counteract the memory-enhancing effects of istradefylline and mediate the worsening of probe performance at higher doses.

$A_{2A}Rs$ may also regulate locomotion and affect neuronal health by distinct mechanisms[34, 53], including through effects on presynaptic and postsynaptic neuronal activities and on glial functions[8, 34,60–64]. In addition, short-term pharmacological blockade is likely to induce a distinct set of biological effects than chronic genetic ablation of the receptor, due to differences in how receptor function is affected and what compensatory and feedback mechanisms are activated in each scenario. Lastly, the presence and extent of neuropathological alterations may have a strong impact on the overall effect of modulating $A_{2A}Rs$.

In young hAPP mice without prominent plaque deposition or astrogliosis, knockdown of $A_{2A}Rs$ in CA3 neurons reduced deficits in synaptic plasticity[12]. Ablation of $A_{2A}Rs$ in excitatory forebrain neurons did not enhance reference memory in mice without hAPP

expression[59, 65], but reduced learning and memory deficits in a model of chronic stress[65]. In addition, optogenetic activation of chimeric A_{2A}Rs in excitatory neurons impaired working memory[66]. Like humans with AD, aging hAPP mice have prominent plaque pathology and marked increases in A_{2A}R expression. In this AD-relevant context, both genetic ablation of A_{2A}Rs in astrocytes[8] and low-dose istradefylline treatment (this study) reduced memory problems. Thus, the specific effects of A_{2A}R ablation or blockade are likely determined by the most prominently affected cell populations and by neuropathological processes that alter A_{2A}R distribution and activity in different cell types. Additional studies are needed to unravel the mechanisms of these differential effects and to explore the therapeutic potential of A_{2A}R antagonists in AD and related conditions.

Supplementary Material

Refer to Web version on PubMed Central for supplementary material.

Acknowledgments

References

1. Schwarzschild MA, Agnati L, Fuxe K, et al. Targeting adenosine A_{2A} receptors in Parkinson's disease. Trends Neurosci. 2006; 29:647–654. [PubMed: 17030429]

2. Kondo T, Mizuno Y, Japanese Istradefylline Study Group. A long-term study of istradefylline safety and efficacy in patients with Parkinson disease. Clin Neuropharmacol. 2015; 38:41–46. [PubMed: 25768849]

3. Pinna A. Adenosine A_{2A} receptor antagonists in Parkinson's disease: Progress in clinical trials from the newly approved istradefylline to drugs in early development and those already discontinued. CNS Drugs. 2014; 28:455–474. [PubMed: 24687255]

4. Cognato GP, Agostinho PM, Hockemeyer J, et al. Caffeine and an adenosine A_{2A} receptor antagonist prevent memory impairment and synaptotoxicity in adult rats triggered by a convulsive episode in early life. J Neurochem. 2010; 112:453–462. [PubMed: 19878534]

5. Ning YL, Yang N, Chen X, et al. Adenosine A2A receptor deficiency alleviates blast-induced cognitive dysfunction. J Cereb Blood Flow Metab. 2013; 33:1789–1798. [PubMed: 23921902]

6. Cunha GM, Canas PM, Melo CS, et al. Adenosine A_{2A} receptor blockade prevents memory dysfunction caused by β-amyloid peptides but not by scopolamine or MK-801. Exp Neurol. 2008; 210:776–781. [PubMed: 18191838]

7. Laurent C, Burnouf S, Ferry B, et al. A_{2A} adenosine receptor deletion is protective in a mouse model of Tauopathy. Mol Psychiatry. 2016; 21:149. [PubMed: 26216297]

8. Orr AG, Hsiao EC, Wang MM, et al. Astrocytic adenosine receptor A_{2A} and G_s-coupled signaling regulate memory. Nat Neurosci. 2015; 18:423–434. [PubMed: 25622143]

9. Dall'Igna OP, Fett P, Gomes MW, et al. Caffeine and adenosine A_{2a} receptor antagonists prevent β-amyloid (25–35)-induced cognitive deficits in mice. Exp Neurol. 2007; 203:241–245. [PubMed: 17007839]

10. Canas PM, Porciuncula LO, Cunha GM, et al. Adenosine A_{2A} receptor blockade prevents synaptotoxicity and memory dysfunction caused by β-amyloid peptides via p38 mitogen-activated protein kinase pathway. J Neurosci. 2009; 29:14741–14751. [PubMed: 19940169]

11. Espinosa J, Rocha A, Nunes F, et al. Caffeine consumption prevents memory impairment, neuronal damage, and adenosine A_{2A} receptors upregulation in the hippocampus of a rat model of sporadic dementia. J Alzheimer's Dis. 2013; 34:509–518. [PubMed: 23241554]

12. Viana da Silva S, Haberl MG, Zhang P, et al. Early synaptic deficits in the APP/PS1 mouse model of Alzheimer's disease involve neuronal adenosine A_{2A} receptors. Nat Commun. 2016; 7:11915. [PubMed: 27312972]

13. Zhang B, Gaiteri C, Bodea LG, et al. Integrated systems approach identifies genetic nodes and networks in late-onset Alzheimer's disease. Cell. 2013; 153:707–720. [PubMed: 23622250]

14. Matos M, Shen HY, Augusto E, et al. Deletion of adenosine A_{2A} receptors from astrocytes disrupts glutamate homeostasis leading to psychomotor and cognitive impairment: Relevance to schizophrenia. Biol Psychiatry. 2015; 78:763–774. [PubMed: 25869810]

15. Ransom BR, Ransom CB. Astrocytes: Multitalented stars of the central nervous system. Methods Mol Biol. 2012; 814:3–7. [PubMed: 22144296]

16. Mucke L, Masliah E, Yu G-Q, et al. High-level neuronal expression of $A\beta_{1-42}$ in wild-type human amyloid protein precursor transgenic mice: Synaptotoxicity without plaque formation. J Neurosci. 2000; 20:4050–4058. [PubMed: 10818140]

17. Palop JJ, Chin J, Roberson ED, et al. Aberrant excitatory neuronal activity and compensatory remodeling of inhibitory hippocampal circuits in mouse models of Alzheimer's disease. Neuron. 2007; 55:697–711. [PubMed: 17785178]

18. Saito T, Matsuba Y, Mihira N, et al. Single App knock-in mouse models of Alzheimer's disease. Nat Neurosci. 2014; 17:661–663. [PubMed: 24728269]

19. Kaye TS, Egorin MJ, Riggs CE Jr, et al. The plasma pharmacokinetics and tissue distribution of dimethyl sulfoxide in mice. Life Sci. 1983; 33:1223–1230. [PubMed: 6888176]

20. Julien C, Marcouiller F, Bretteville A, et al. Dimethyl sulfoxide induces both direct and indirect tau hyperphosphorylation. PLoS One. 2012; 7:e40020. [PubMed: 22768202]

21. Yang M, Soohoo D, Soelaiman S, et al. Characterization of the potency, selectivity, and pharmacokinetic profile for six adenosine A_{2A} receptor antagonists. Naunyn-Schmiedeberg's Arch Pharmacol. 2007; 375:133–144. [PubMed: 17310264]

22. Hockemeyer J, Burbiel JC, Muller CE. Multigram-scale syntheses, stability, and photoreactions of A_{2A} adenosine receptor antagonists with 8-styrylxanthine structure: Potential drugs for Parkinson's disease. J Org Chem. 2004; 69:3308–3318. [PubMed: 15132536]

23. Muller CE, Geis U, Hipp J, et al. Synthesis and structure-activity relationships of 3,7-dimethyl-1-propargylxanthine derivatives, A_{2A}-selective adenosine receptor antagonists. J Med Chem. 1997; 40:4396–4405. [PubMed: 9435909]

24. Gordon MN, Osterburg HH, May PC, et al. Effective oral administration of 17 β-estradiol to female C57BL/6J mice through the drinking water. Biol Reprod. 1986; 35:1088–1095. [PubMed: 3828426]

25. Possin KL, Sanchez PE, Anderson-Bergman C, et al. Cross-species translation of the Morris maze for Alzheimer's disease. J Clin Invest. 2016; 126:779–783. [PubMed: 26784542]

26. R Development Core Team. R: A language and environment for statistical computing. Vienna, Austria: R Foundation for Statistical Computing; 2015.

27. Palop JJ, Mucke L. Network abnormalities and interneuron dysfunction in Alzheimer disease. Nat Rev Neurosci. 2016; 17:777–792. [PubMed: 27829687]

28. Musiek ES, Holtzman DM. Three dimensions of the amyloid hypothesis: Time, space and 'wingmen'. Nat Neurosci. 2015; 18:800–806. [PubMed: 26007213]

29. Serrano-Pozo A, Betensky RA, Frosch MP, et al. Plaque-associated local toxicity increases over the clinical course of Alzheimer disease. Am J Pathol. 2016; 186:375–384. [PubMed: 26687817]

30. Mrak RE, Griffin WS. Glia and their cytokines in progression of neurodegeneration. Neurobiol Aging. 2005; 26:349–354. [PubMed: 15639313]

31. Masuda A, Kobayashi Y, Kogo N, et al. Cognitive deficits in single *App* knock-in mouse models. Neurobiol Learn Mem. 2016; 135:73–82. [PubMed: 27377630]

32. Sahlin C, Lord A, Magnusson K, et al. The Arctic Alzheimer mutation favors intracellular amyloid-β production by making amyloid precursor protein less available to α-secretase. J Neurochem. 2007; 101:854–862. [PubMed: 17448150]

33. Matos M, Augusto E, Machado NJ, et al. Astrocytic adenosine A_{2A} receptors control the amyloid-β peptide-induced decrease of glutamate uptake. J Alzheimer's Dis. 2012; 31:555–567. [PubMed: 22647260]

34. Yu L, Shen HY, Coelho JE, et al. Adenosine A_{2A} receptor antagonists exert motor and neuroprotective effects by distinct cellular mechanisms. Ann Neurol. 2008; 63:338–346. [PubMed: 18300283]

35. Bastia E, Xu YH, Scibelli AC, et al. A crucial role for forebrain adenosine A_{2A} receptors in amphetamine sensitization. Neuropsychopharmacology. 2005; 30:891–900. [PubMed: 15602504]

36. Morris RJ. Developments of a water-maze procedure for studying spatial learning in the rat. J Neurosci Methods. 1984; 11:47–60. [PubMed: 6471907]

37. Maei HR, Zaslavsky K, Teixeira CM, et al. What is the most sensitive measure of water maze probe test performance? Front Integr Neurosci. 2009; 3:4. [PubMed: 19404412]

38. Gallagher M, Burwell R, Burchinal M. Severity of spatial learning impairment in aging: Development of a learning index for performance in the Morris water maze. Behav Neurosci. 1993; 107:618–626. [PubMed: 8397866]

39. Rice JP, Wallace DG, Hamilton DA. Lesions of the hippocampus or dorsolateral striatum disrupt distinct aspects of spatial navigation strategies based on proximal and distal information in a cued variant of the Morris water task. Behav Brain Res. 2015; 289:105–117. [PubMed: 25907746]

40. Vianna MR, Alonso M, Viola H, et al. Role of hippocampal signaling pathways in long-term memory formation of a nonassociative learning task in the rat. Learn Mem. 2000; 7:333–340. [PubMed: 11040265]

41. Nikodijevic O, Jacobson KA, Daly JW. Locomotor activity in mice during chronic treatment with caffeine and withdrawal. Pharmacol Biochem Behav. 1993; 44:199–216. [PubMed: 7679219]

42. Kachroo A, Orlando LR, Grandy DK, et al. Interactions between metabotropic glutamate 5 and adenosine A_{2A} receptors in normal and parkinsonian mice. J Neurosci. 2005; 25:10414–10419. [PubMed: 16280580]

43. Wang JH, Ma YY, van den Buuse M. Improved spatial recognition memory in mice lacking adenosine A_{2A} receptors. Exp Neurol. 2006; 199:438–445. [PubMed: 16519887]

44. Baldi E, Bucherelli C. The inverted "u-shaped" dose-effect relationships in learning and memory: Modulation of arousal and consolidation. Nonlinearity Biol Toxicol Med. 2005; 3:9–21. [PubMed: 19330154]

45. Arendash GW, Schleif W, Rezai-Zadeh K, et al. Caffeine protects Alzheimer's mice against cognitive impairment and reduces brain β-amyloid production. Neuroscience. 2006; 142:941–952. [PubMed: 16938404]

46. Cao C, Loewenstein DA, Lin X, et al. High blood caffeine levels in MCI linked to lack of progression to dementia. J Alzheimer's Dis. 2012; 30:559–572. [PubMed: 22430531]

47. Borota D, Murray E, Keceli G, et al. Post-study caffeine administration enhances memory consolidation in humans. Nat Neurosci. 2014; 17:201–203. [PubMed: 24413697]

48. Ko WK, Camus SM, Li Q, et al. An evaluation of istradefylline treatment on Parkinsonian motor and cognitive deficits in 1-methyl-4-phenyl-1,2,3,6-tetrahydropyridine (MPTP)-treated macaque models. Neuropharmacology. 2016; 110:48–58. [PubMed: 27424102]

49. Calabrese EJ. Alzheimer's disease drugs: An application of the hormetic dose-response model. Crit Rev Toxicol. 2008; 38:419–451. [PubMed: 18568864]

50. Jack CR Jr, Holtzman DM. Biomarker modeling of Alzheimer's disease. Neuron. 2013; 80:1347–1358. [PubMed: 24360540]

51. Rissanen E, Virta JR, Paavilainen T, et al. Adenosine A2A receptors in secondary progressive multiple sclerosis: A [11C]TMSX brain PET study. J Cereb Blood Flow Metab. 2013; 33:1394–1401. [PubMed: 23695433]

52. Tavares AA, Batis JC, Papin C, et al. Kinetic modeling, test-retest, and dosimetry of ^{123}I-MNI-420 in humans. J Nucl Med. 2013; 54:1760–1767. [PubMed: 23970369]

53. Chen JF, Sonsalla PK, Pedata F, et al. Adenosine A_{2A} receptors and brain injury: Broad spectrum of neuroprotection, multifaceted actions and "fine tuning" modulation. Prog Neurobiol. 2007; 83:310–331. [PubMed: 18023959]

54. Cunha RA. Neuroprotection by adenosine in the brain: From A_1 receptor activation to A_{2A} receptor blockade. Purinergic Signal. 2005; 1:111–134. [PubMed: 18404497]

55. Popoli P, Pintor A, Domenici MR, et al. Blockade of striatal adenosine A_{2A} receptor reduces, through a presynaptic mechanism, quinolinic acid-induced excitotoxicity: Possible relevance to neuroprotective interventions in neurodegenerative diseases of the striatum. J Neurosci. 2002; 22:1967–1975. [PubMed: 11880527]

56. Blum D, Galas MC, Pintor A, et al. A dual role of adenosine A_{2A} receptors in 3-nitropropionic acid-induced striatal lesions: Implications for the neuroprotective potential of A_{2A} antagonists. J Neurosci. 2003; 23:5361–5369. [PubMed: 12832562]

57. Burnstock G. Physiology and pathophysiology of purinergic neurotransmission. Physiol Rev. 2007; 87:659–797. [PubMed: 17429044]

58. Shen HY, Coelho JE, Ohtsuka N, et al. A critical role of the adenosine A_{2A} receptor in extrastriatal neurons in modulating psychomotor activity as revealed by opposite phenotypes of striatum and forebrain A_{2A} receptor knock-outs. J Neurosci. 2008; 28:2970–2975. [PubMed: 18354001]

59. Wei CJ, Singer P, Coelho J, et al. Selective inactivation of adenosine A_{2A} receptors in striatal neurons enhances working memory and reversal learning. Learn Mem. 2011; 18:459–474. [PubMed: 21693634]

60. Shen HY, Canas PM, Garcia-Sanz P, et al. Adenosine A_2A receptors in striatal glutamatergic terminals and GABAergic neurons oppositely modulate psychostimulant action and DARPP-32 phosphorylation. PLoS One. 2013; 8:e80902. [PubMed: 24312250]

61. Orr AG, Orr AL, Li XJ, et al. Adenosine A_{2A} receptor mediates microglial process retraction. Nat Neurosci. 2009; 12:872–878. [PubMed: 19525944]

62. Rebola N, Simões AP, Canas PM, et al. Adenosine A_{2A} receptors control neuroinflammation and consequent hippocampal neuronal dysfunction. J Neurochem. 2011; 117:100–111. [PubMed: 21235574]

63. Gyoneva S, Shapiro L, Lazo C, et al. Adenosine A_{2A} receptor antagonism reverses inflammation-induced impairment of microglial process extension in a model of Parkinson's disease. Neurobiol Dis. 2014; 67:191–202. [PubMed: 24632419]

64. Madeira MH, Boia R, Elvas F, et al. Selective A_{2A} receptor antagonist prevents microglia-mediated neuroinflammation and protects retinal ganglion cells from high intraocular pressure-induced transient ischemic injury. Transl Res. 2016; 169:112–128. [PubMed: 26685039]

65. Kaster MP, Machado NJ, Silva HB, et al. Caffeine acts through neuronal adenosine A_{2A} receptors to prevent mood and memory dysfunction triggered by chronic stress. Proc Natl Acad Sci USA. 2015; 112:7833–7838. [PubMed: 26056314]

66. Li P, Rial D, Canas PM, et al. Optogenetic activation of intracellular adenosine A_{2A} receptor signaling in the hippocampus is sufficient to trigger CREB phosphorylation and impair memory. Mol Psychiatry. 2015; 20:1339–1349. [PubMed: 25687775]

Highlights

- A_{2A} receptors on astrocytes may contribute to memory loss in Alzheimer's disease

- Amyloid plaque pathology but not APP overexpression increases astrocytic A_{2A} levels

- Istradefylline is a safe and selective A_{2A} receptor blocker used in the clinic

- Low-dose istradefylline enhances spatial memory in aging mice with plaque pathology

- Low-dose istradefylline does not affect movement or increase anxiety in aging mice
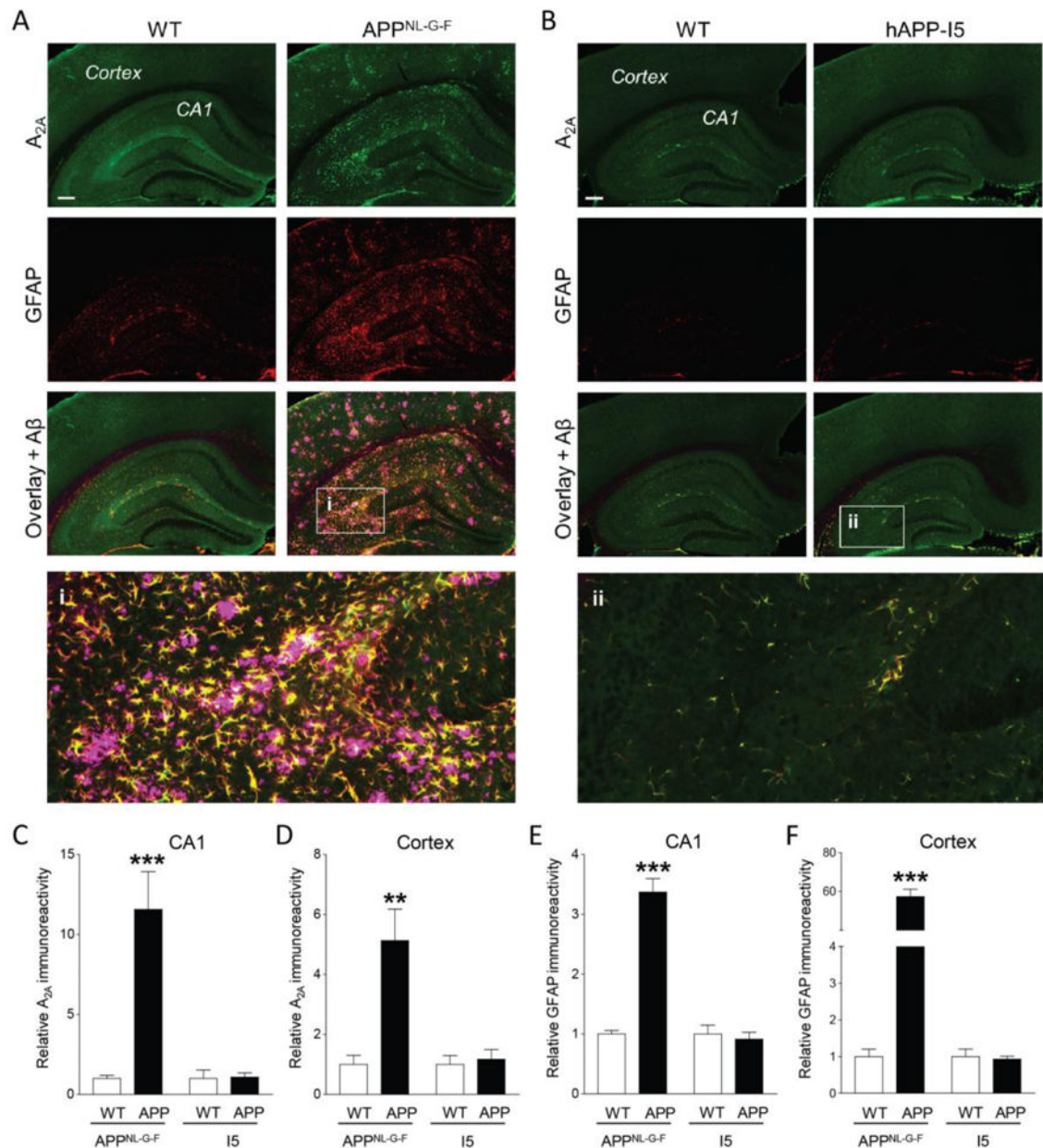
Fig. 1. Increases in A$_{2A}$ levels in mice with amyloid-β accumulation

(A and B) Representative photomicrographs of hippocampal and neocortical sections from 9–10-month-old APP^{NL-G-F} (A) and hAPP-I5 (B) mice and age-matched wildtype (WT) controls (A and B) immunostained for the A$_{2A}$R (green), GFAP (red) and Aβ (magenta). Overlay of A$_{2A}$R and GFAP is shown in yellow. Insets (i–ii) show magnified views of the boxed regions. Scale bars: 200 μm. (C–F) Levels of A$_{2A}$R and GFAP immunoreactivities in CA1 and neocortex normalized to total selected brain areas and averages in WT littermates. A$_{2A}$R: n=4 WT mice (from APP^{NL-G-F} line), 14 APP^{NL-G-F} mice, 6 WT mice (from hAPP-I5 line), 15 hAPP-I5 mice. GFAP: n=4 WT mice (APP^{NL-G-F} line), 9 APP^{NL-G-F} mice, 6 WT mice (hAPP-I5 line), 10 hAPP-I5 mice. **P<0.01, ***P<0.001 vs. WT littermate controls (t test with Welch's correction). Values are means ± SEM.
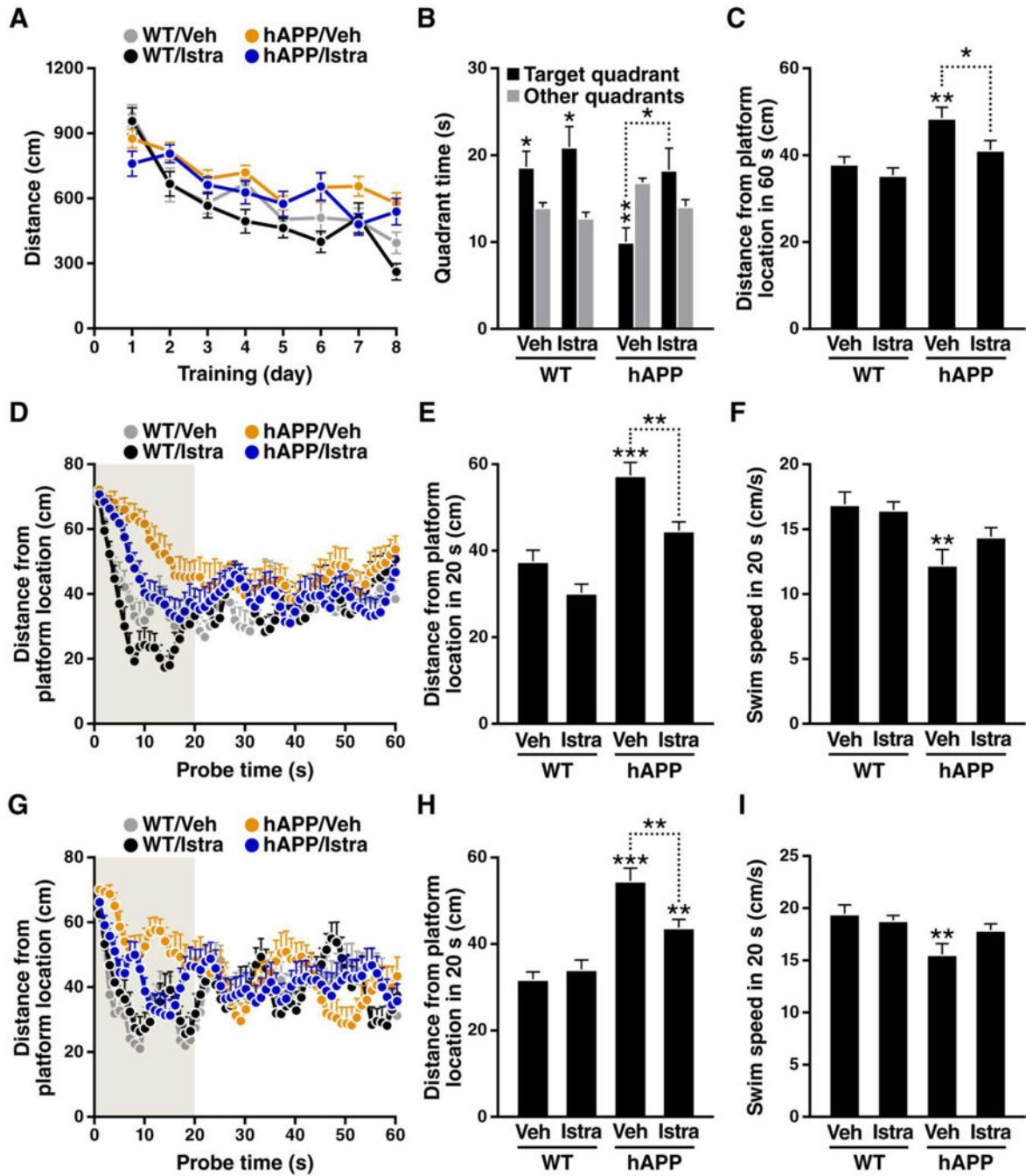
Fig. 2. Istradefylline enhances spatial memory in hAPP mice

14–15-month-old WT and hAPP-J20 mice treated with vehicle (Veh) or istradefylline (Istra, 10 mg/kg/day) were tested in the Morris water maze. (A) Distance traveled during hidden platform training (four trials/day). Linear regression analysis: t=2.966, P=0.0045 for genotype effect; t=−1.583, P=0.112 for drug effect; t=−0.019, P=0.99 for interaction effect. n=14–16 mice per genotype and treatment. (B–I) Probe trials 1 day (B–F) and 3 days (G–I) after training. (B) Time in target and nontarget (other) quadrants. Two-way ANOVA of target quadrant time: $F(1,52)$=5.66, P=0.0211 for drug effect; $F(1,52)$=6.42, P=0.0143 for

genotype effect. *t* test with FDR correction for multiple comparisons (target vs. other quadrants): *P*=0.044 (WT/Veh), 0.012 (WT/Istra), 0.008 (hAPP/Veh), 0.14 (hAPP/Istra). *n*=13–15 mice per genotype and treatment. (C–E) Distance from the platform location. Average distance in 60 seconds (C–D) and the first 20 seconds (E) of the 24-hour probe trial. Two-way ANOVA: (C) *F*(1,53)=4.93, *P*=0.0307 for drug effect; *F*(1,53)=13.37, *P*=0.0006 for genotype effect. *n*=13–16 mice per genotype and treatment. (E) *F*(1,51)=14.46, *P*=0.0004 for drug effect; *F*(1,51)=42.22, *P*<0.0001 for genotype effect. *n*=3–15 mice per genotype and treatment. (F) Swim speed. Two-way ANOVA: *F*(1,52)=12.40, *P*=0.0009 for genotype effect. *n*=14–16 mice per genotype and treatment. (G and H) Distance from the platform location. Average distance in 60 seconds (G) and the first 20 seconds (H) of the 72-hour probe trial. Two-way ANOVA: (H) *F*(1,52)=7.20, *P*=0.0098 for interaction effect; *F*(1,52)=44.54, *P*<0.0001 for genotype effect. *n*=13–16 mice per genotype and treatment. (I) Swim speed. Two-way ANOVA: *F*(1,53)=8.30, *P*=0.0057 for genotype effect. *n*=13–16 mice per genotype and treatment. *P<0.05, **P<0.01, ***P<0.001 vs. other quadrants by *t* test (B) or WT/Veh group by Dunnett's test (C, E, F, H, I), or as indicated by the brackets (Bonferroni test). Green shading indicates the first 20 seconds of the probe trial. Values are means ± SEM.